

Well Developed Deformation in  $^{42}\text{Si}$ 

S. Takeuchi,<sup>1,\*</sup> M. Matsushita,<sup>1,2,†</sup> N. Aoi,<sup>1,‡</sup> P. Doornenbal,<sup>1</sup> K. Li,<sup>1,3</sup> T. Motobayashi,<sup>1</sup> H. Scheit,<sup>1,§</sup> D. Steppenbeck,<sup>1,†</sup> H. Wang,<sup>1,3</sup> H. Baba,<sup>1</sup> D. Bazin,<sup>4</sup> L. C aceres,<sup>5</sup> H. Crawford,<sup>6</sup> P. Fallon,<sup>6</sup> R. Gernh user,<sup>7</sup> J. Gibelin,<sup>8</sup> S. Go,<sup>9</sup> S. Gr vy,<sup>5</sup> C. Hinke,<sup>7</sup> C. R. Hoffman,<sup>10</sup> R. Hughes,<sup>11</sup> E. Ideguchi,<sup>9,‡</sup> D. Jenkins,<sup>12</sup> N. Kobayashi,<sup>13</sup> Y. Kondo,<sup>13</sup> R. Kr ucken,<sup>7,||</sup> T. Le Bleis,<sup>14,15,¶</sup> J. Lee,<sup>1</sup> G. Lee,<sup>13</sup> A. Matta,<sup>16</sup> S. Michimasa,<sup>9</sup> T. Nakamura,<sup>13</sup> S. Ota,<sup>9</sup> M. Petri,<sup>6,§</sup> T. Sako,<sup>13</sup> H. Sakurai,<sup>1</sup> S. Shimoura,<sup>9</sup> K. Steiger,<sup>7</sup> K. Takahashi,<sup>13</sup> M. Takechi,<sup>1,\*\*</sup> Y. Togano,<sup>1,\*\*</sup> R. Winkler,<sup>4,††</sup> and K. Yoneda<sup>1</sup>

<sup>1</sup>RIKEN Nishina Center, Wako, Saitama 351-0198, Japan

<sup>2</sup>Department of Physics, Rikkyo University, Toshima, Tokyo 172-8501, Japan

<sup>3</sup>Peking University, Beijing 100871, People's Republic of China

<sup>4</sup>National Superconducting Cyclotron Laboratory, Michigan State University, East Lansing, Michigan 48824, USA

<sup>5</sup>Grand Acc el rateur National d'Ions Lourds, CEA/DSM-CNRS/IN2P3, F-14076 Caen Cedex 5, France

<sup>6</sup>Lawrence Berkeley National Laboratory, Berkeley, California 94720, USA

<sup>7</sup>Physik Department, Technische Universit t M nchen, D-85748 Garching, Germany

<sup>8</sup>LPC-ENSICAEN, IN2P3-CNRS et Universit  de Caen, F-14050, Caen Cedex, France

<sup>9</sup>Center for Nuclear Study, University of Tokyo, RIKEN campus, Wako, Saitama 351-0198, Japan

<sup>10</sup>Physics Division, Argonne National Laboratory, Argonne, Illinois 60439, USA

<sup>11</sup>Department of Physics, University of Richmond, Richmond, Virginia 23173, USA

<sup>12</sup>Physics Department, University of York, Heslington, York YO10 5DD, United Kingdom

<sup>13</sup>Department of Physics, Tokyo Institute of Technology, Meguro, Tokyo 152-8551, Japan

<sup>14</sup>Institut f r Kernphysik, Johann-Wolfgang-Goethe-Universit t, D-60486 Frankfurt, Germany

<sup>15</sup>GSI Helmholtzzentrum f r Schwerionenforschung D-64291 Darmstadt, Germany

<sup>16</sup>Institut de Physique Nucl aire, IN2P3-CNRS, Universit  de Paris Sud, F-91406 Orsay, France

(Received 26 July 2012; revised manuscript received 19 September 2012; published 2 November 2012)

Excited states in  $^{38,40,42}\text{Si}$  nuclei have been studied via in-beam  $\gamma$ -ray spectroscopy with multinucleon removal reactions. Intense radioactive beams of  $^{40}\text{S}$  and  $^{44}\text{S}$  provided at the new facility of the RIKEN Radioactive Isotope Beam Factory enabled  $\gamma$ - $\gamma$  coincidence measurements. A prominent  $\gamma$  line observed with an energy of 742(8) keV in  $^{42}\text{Si}$  confirms the  $2^+$  state reported in an earlier study. Among the  $\gamma$  lines observed in coincidence with the  $2^+ \rightarrow 0^+$  transition, the most probable candidate for the transition from the yrast  $4^+$  state was identified, leading to a  $4_1^+$  energy of 2173(14) keV. The energy ratio of 2.93(5) between the  $2_1^+$  and  $4_1^+$  states indicates well-developed deformation in  $^{42}\text{Si}$  at  $N = 28$  and  $Z = 14$ . Also for  $^{38,40}\text{Si}$  energy ratios with values of 2.09(5) and 2.56(5) were obtained. Together with the ratio for  $^{42}\text{Si}$ , the results show a rapid deformation development of Si isotopes from  $N = 24$  to  $N = 28$ .

DOI: 10.1103/PhysRevLett.109.182501

PACS numbers: 25.60.-t, 23.20.Lv, 27.40.+z, 29.38.Db

Shell closures and collectivity are important properties that characterize the atomic nucleus. Interchange of their dominance along isotopic or isotonic chains has attracted much attention. The recent extension of the research frontier to nuclei far away from the valley of stability has revealed several new phenomena for neutron- or proton-number dependent nuclear structure. For example, a weakening or even disappearance of shell closures occurs in several neutron-rich nuclei at  $N = 8$  [1–3] and  $N = 20$  [4–6]. A well-known example in the case of  $N = 20$  is the so-called ‘‘island of inversion’’ [7] located around the neutron-rich nucleus  $^{32}\text{Mg}$ . The low excitation energy of the first  $2^+$  state  $E_x(2_1^+)$  and large  $E2$  transition probability [4–6] clearly indicate shell quenching in  $^{32}\text{Mg}$  despite the fact that  $N = 20$  is traditionally a magic number. The next magic number,  $N = 28$ , which appears due to the  $f_{7/2} - f_{5/2}$  spin-orbit splitting, has also been explored [8–13]. Weakening of the shell closure is seen by the decrease of the  $2_1^+$  energy for  $N = 28$  isotones from

3.83 MeV in the doubly closed nucleus  $^{48}\text{Ca}$  to 1.33 MeV in  $^{44}\text{S}$  as the proton number decreases from  $Z = 20$  to  $Z = 16$ . Another region of shell stability has been shown to exist at  $N, Z = 14$  due to the  $d_{5/2} - d_{3/2}$  spin-orbit splitting. The silicon isotopes from  $^{28}\text{Si}$  to  $^{34}\text{Si}$  exhibit relatively high  $2_1^+$  energies ranging from 1.78 MeV ( $^{28}\text{Si}$ ) to 3.33 MeV ( $^{34}\text{Si}$ ) reflecting the  $Z = 14$  subshell closure. However, the  $2_1^+$  energy gradually decreases from  $^{36}\text{Si}$  to  $^{40}\text{Si}$  [12,14], suggesting a development of quadrupole collectivity for isotopes with  $N > 20$ .

With proton number  $Z = 14$  and neutron number  $N = 28$ , the nuclear structure of  $^{42}\text{Si}$  is of special interest. A simple but important question that arises is whether the weakening of the  $N = 28$  shell closure continues, causing an enhancement of nuclear collectivity, or if shell stability is restored owing to a possible doubly magic structure. An experimental study on  $^{42}\text{Si}$  was done using a two-proton removal reaction with a radioactive  $^{44}\text{S}$  beam at the National Superconducting Cyclotron Laboratory [15].

The small two-proton removal cross section was interpreted as evidence for a large  $Z = 14$  subshell gap at  $N = 28$ , indicating a nearly spherical shape and a doubly closed-shell structure for  $^{42}\text{Si}$ . Contrary to this result, a disappearance of the  $N = 28$  spherical shell closure around  $^{42}\text{Si}$  was concluded by another experimental study at Grand Accélérateur National d'Ions Lourds with the same reaction [16] owing to the observation of a low-energy  $\gamma$  line interpreted as the transition from the  $2_1^+$  state at 770(19) keV to the ground  $0^+$  state ( $0_{g.s.}^+$ ). This low  $E_x(2_1^+)$  value supports the nonmagic nature of  $^{42}\text{Si}$  expected from comparison of the  $\beta$ -decay half-life of  $^{42}\text{Si}$  with quasiparticle random-phase approximation calculations [11].

The disappearance of the  $N = 28$  shell closure for  $^{42}\text{Si}$  was theoretically pointed out in several recent studies with shell-model and mean-field approaches [17–19]. These studies predict a well-developed large deformation of the ground and low-lying states. For further understanding of the structure of  $^{42}\text{Si}$  and, more generally, the mechanism of interchange between the shell closures and quadrupole collectivity along the  $N = 28$  and  $Z = 14$  chains, further experimental input is necessary. In addition to the energy of the  $2_1^+$  state, the location of the  $4_1^+$  state is of crucial importance, since the energy ratio between the  $4_1^+$  and  $2_1^+$  states ( $R_{4/2}$ ) represents the character of quadrupole collectivity: a ratio of 2 is expected for harmonic vibration and 3.33 for rigid-body rotation, as extremes. Hence, the systematic study of  $E_x(2_1^+)$  and  $E_x(4_1^+)$  values is useful to deepen our understanding of the mechanism for the evolution of nuclear structure in the vicinity of  $^{42}\text{Si}$ .

The purpose of the present study is to find the  $4_1^+$  state in  $^{42}\text{Si}$  as well as to revisit the  $2_1^+ \rightarrow 0_{g.s.}^+$  transition. Owing to the secondary  $^{44}\text{S}$  beam with the world's highest intensity provided by the RIKEN Radioactive Isotope Beam Factory (RIBF), population of the  $4_1^+$  state in  $^{42}\text{Si}$  by the two-proton removal reaction was possible, and even a  $\gamma - \gamma$  coincidence analysis was enabled to establish the level scheme with the help of the high-efficiency detector array DALI2 (Detector Array for Low-Intensity radiation 2) [20,21]. Additionally, we studied multinucleon removal reactions of  $^{44}\text{S}$  and  $^{40}\text{S}$  to populate  $4^+$  states in  $^{40}\text{Si}$  and  $^{38}\text{Si}$  in order to obtain valuable information on the evolution of the quadrupole collectivity in neutron-rich Si isotopes provided by the systematic trend of the ratio  $R_{4/2}$ .

The experiment was performed at the RIBF operated by RIKEN Nishina Center and the Center for Nuclear Study, University of Tokyo. A primary  $^{48}\text{Ca}$  beam at 345 MeV/nucleon with an average intensity of 70 pA bombarded a 15-mm-thick rotating beryllium target. A secondary  $^{44}\text{S}$  or  $^{40}\text{S}$  beam was produced by projectile fragmentation and analyzed by the BigRIPS fragment separator [22] as in earlier experiments [23,24]. The energy and intensity of the secondary  $^{44}\text{S}$  ( $^{40}\text{S}$ ) beam was approximately 210 MeV/nucleon (210 MeV/nucleon)

and  $4 \times 10^4$  particles per second (pps) ( $6 \times 10^4$  pps), respectively.

A carbon target with a thickness of 2.54 g/cm<sup>2</sup> was located at the F8 focus for secondary reactions. Reaction products were analyzed using the ZeroDegree spectrometer [25], and identified using the energy loss ( $\Delta E$ ), magnetic rigidity ( $B\rho$ ), and time-of-flight information. The  $B\rho$  value was obtained from the position at the dispersive focus F9 measured by parallel plate avalanche counters [26].  $\Delta E$  was measured by an ionization chamber at the achromatic focus F11 and the time-of-flight information was obtained from the time difference between plastic scintillators at F8 and F11. The inclusive cross section for the  $\text{C}(^{44}\text{S}, ^{42}\text{Si})$  reaction at 210 MeV/nucleon was found to be 0.15(2) mb, which indicates a monotonic rise of the cross section as compared with 0.12(2) mb at 98.6 MeV/nucleon [15] and 0.08(1) mb at 39 MeV/nucleon [16].

De-excitation  $\gamma$  rays were detected by the DALI2 array in coincidence with the outgoing  $^{42}\text{Si}$ ,  $^{40}\text{Si}$ , and  $^{38}\text{Si}$  particles. DALI2 consists of 186 NaI(Tl) detectors surrounding the reaction target that cover an angular range of  $11^\circ$ – $160^\circ$  with respect to the beam axis. The typical photopeak efficiency and energy resolution are 20% and 10% (full width at half maximum), respectively, for 1 MeV  $\gamma$  rays emitted from nuclei moving with  $\beta(=v/c) \approx 0.6$ . These values were obtained by Monte Carlo simulations using the GEANT4 code [27].

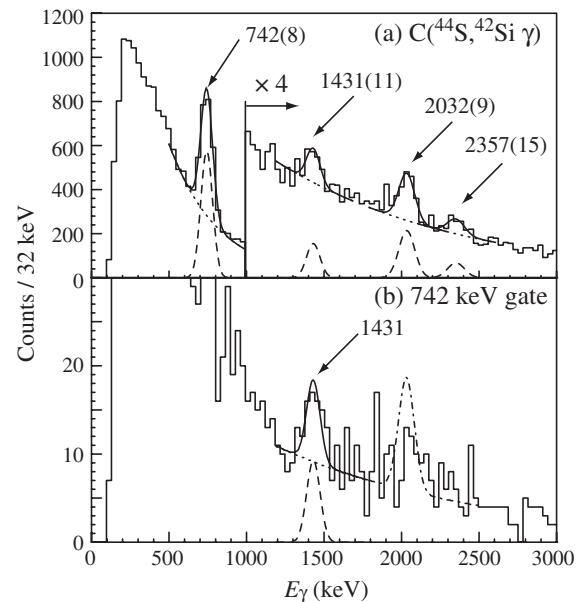


FIG. 1. (a) Doppler-shift corrected  $\gamma$ -ray spectrum obtained for the  $\text{C}(^{44}\text{S}, ^{42}\text{Si})\gamma$  reaction. (b)  $\gamma - \gamma$  coincidence spectrum gated with the 742 keV  $\gamma$  ray. Solid curves in both figures show the results of fits using Gaussian functions (dashed curves) and an exponential curve as the background (dotted curve) by the  $\chi^2$  minimization method. The dot-dashed line indicates the expected line shape in the case that the 2032-keV  $\gamma$  ray decays solely to the  $2^+$  state.

Figure 1(a) shows the Doppler-corrected  $\gamma$ -ray energy spectrum for the  $C(^{44}\text{S}, ^{42}\text{Si}\gamma)$  reaction. For each  $\gamma$ -ray peak, the energy was obtained by a fit of a Gaussian function and an exponential background curve, where the energy resolution was fixed to the simulated value. As seen in the figure, a predominant peak is observed at 742(8) keV, where the error includes statistical and systematic uncertainties. The systematic error is attributed to the uncertainties in the energy calibration (3 keV), the Doppler-shift correction (3 keV), and the ambiguity caused by a delay of  $\gamma$  emission resulting in a shift of the source position (estimated to be 2 keV as a maximum lifetime of  $\sim 40$  ps based on systematics [28]). The observed peak energy agrees within 1.5 standard deviations with the value of 770(19) keV reported in the study at Grand Accélérateur National d'Ions Lourds [16]. In the higher energy region, three additional  $\gamma$  lines have been identified in the present study at 1431(11), 2032(9), and 2357(15) keV.

In order to identify the transitions feeding the  $2_1^+$  state, a  $\gamma - \gamma$  coincidence analysis was performed. The spectrum obtained from a gate on the 742-keV line is shown in Fig. 1(b). A clear peak is seen at 1431 keV, which may feed the  $2_1^+$  state directly from a higher-lying excited state at 2173(14) keV. By considering the  $\gamma$ -ray detection efficiency, the yield of the peak is consistent with a 100% feeding of the  $2_1^+$  state. A peaklike structure around  $E_\gamma \approx 2$  MeV could correspond to the 2032-keV  $\gamma$  line observed in Fig. 1(a), providing another candidate that populates the  $2_1^+$  state. However, the yield of the peak in the  $\gamma - \gamma$  spectrum is lower than the expected value (indicated by the dot-dashed line), based on the intensity measured in Fig. 1(a) and assuming a decay branch of 100% to the level at 742 keV. This suggests that the 2032-keV  $\gamma$  ray does not, or at least does not fully, populate the  $2_1^+$  state. From the known tendency that yrast states, including the  $2_1^+$  and  $4_1^+$  states, are preferentially observed with larger cross sections in nucleon removal reactions [29–31], those two  $\gamma$  lines are possible candidates for the  $4_1^+ \rightarrow 2_1^+$  transition in  $^{42}\text{Si}$ . Since the  $\gamma - \gamma$  coincidence analysis indicates that the 1431-keV  $\gamma$  ray directly feeds the  $2_1^+$  state as discussed above, 2173 (742 + 1431) keV for the  $4_1^+$  energy is more probable among the two possibilities. Thus, we tentatively assign the  $4_1^+$  state at 2173(14) keV. The resultant  $R_{4/2}$  value of 2.93(5) for  $^{42}\text{Si}$  is rather close to the rigid-rotor limit. This contradicts the possibility of a doubly closed structure suggested by the two magic numbers  $Z = 14$  and  $N = 28$ , but supports enhanced quadrupole collectivity in  $^{42}\text{Si}$  expected from the measured  $2_1^+$  energy [16] and theoretical calculations [17–19]. Furthermore, the large  $R_{4/2}$  value indicates a large static ground state deformation of  $^{42}\text{Si}$ .

A search for  $4_1^+$  states in  $^{38,40}\text{Si}$  was also conducted. Figures 2(a) and 2(b) show the Doppler-corrected spectra for  $^{38}\text{Si}$  and  $^{40}\text{Si}$ , measured with the  $C(^{40}\text{S}, ^{38}\text{Si}\gamma)$  and  $C(^{44}\text{S}, ^{40}\text{Si}\gamma)$  reactions, respectively. In the case of  $^{38}\text{Si}$ ,

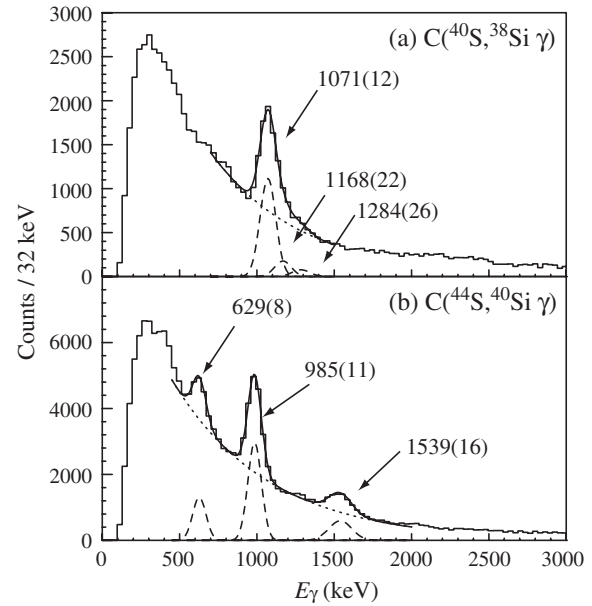


FIG. 2. Doppler-shift corrected  $\gamma$ -ray spectrum obtained in (a) the  $C(^{40}\text{S}, ^{38}\text{Si}\gamma)$  reaction and (b) the  $C(^{44}\text{S}, ^{40}\text{Si}\gamma)$  reaction.

the major peak likely consists of three unresolved  $\gamma$ -ray lines, according to the ones observed in a previous experiment [13]. Their energies, 1071(12), 1168(22), and 1284(26) keV, were obtained by fitting the spectrum shown in Fig. 2(a), where three peaks with fixed widths and initial centroid positions estimated from Ref. [13] were used in the fitting procedure. The 1071-keV  $\gamma$  line corresponds to the known  $2_1^+ \rightarrow 0_{g.s.}^+$  transition, while the 1168- and 1284-keV lines are candidates for the  $4_1^+ \rightarrow 2_1^+$   $\gamma$  ray. Here, we assign the 2239-keV state to be the most probable candidate for the  $4_1^+$  state, based on the same arguments of yrast feeding that were discussed for  $^{42}\text{Si}$ . We note that the alternative  $4_1^+$  assignment to the 2355-keV state does not affect the discussion on the systematics of the level energies of Si isotopes discussed later.

For  $^{40}\text{Si}$ , three  $\gamma$  lines are seen at 629(8), 985(11), and 1539(16) keV in Fig. 2(b). The 629- and 985-keV lines have been observed in the  $p(^{42}\text{P}, ^{40}\text{Si} + \gamma)$  reaction. The 985-keV  $\gamma$  ray was assigned to the  $2_1^+ \rightarrow 0_{g.s.}^+$  transition [12]. The line at 1539 keV is reported here for the first time. According to  $\gamma - \gamma$  coincidence analysis, the 629- and 1539-keV  $\gamma$  lines are considered to be transitions from the excited states at 1614(14) and 2524(19) keV to the  $2_1^+$  state. Using similar arguments to those given for  $^{38}\text{Si}$  and  $^{42}\text{Si}$  regarding the preferential population of yrast states, either of the two states could be the yrast  $4^+$  level. However, systematic trends of  $2^+$  and  $4^+$  energies suggest that the level at 2524 keV is the more likely of the two. The 1614-keV state is consistent with the previously observed tentative 1624(7)-keV state [12]. On the basis of the large-scale shell model (SM) calculations in a  $\pi(sd)^{Z-8}\nu(pf)^{N-20}$  model space [12] this level could be either a  $0^+$  or  $2^+$  level.

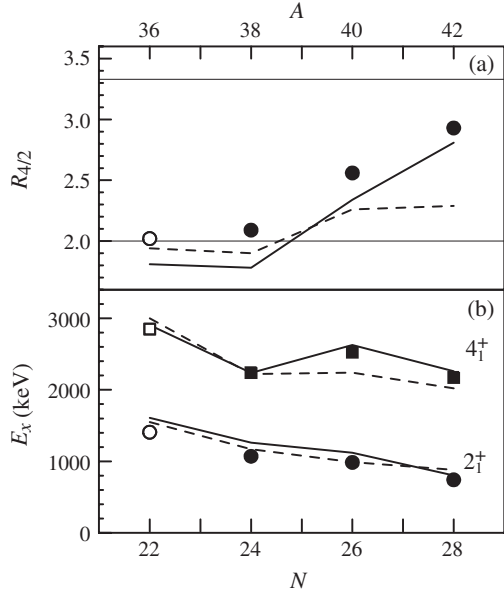


FIG. 3. (a) Ratio between the energies of the  $2_1^+$  and  $4_1^+$  states ( $R_{4/2}$ ) for Si isotopes. The horizontal lines at 2.0 and 3.3 indicate the vibrational and rotational limits, respectively. (b) Excitation energies for  $2_1^+$  and  $4_1^+$  states, which are indicated by circles and squares, respectively. Filled symbols are results of the present study, and solid and dashed lines represent predictions of the SM with SDPF-MU [17] and SM with SDPF-U-MIX [33], respectively (see text for details). The  $2^+$  energies of the  $N = 24, 26, 28$  Si isotopes have been measured in previous works [12,14,16].

Figure 3 shows the isotopic dependence of the excitation energies of the  $2_1^+$  and  $4_1^+$  states together with their ratio  $R_{4/2}$  for  $^{36-42}\text{Si}$ , where filled symbols represent the present results, and open symbols for  $^{36}\text{Si}$  are taken from Ref. [32]. As seen in the figure, the ratios for  $^{36}\text{Si}$  and  $^{38}\text{Si}$  [ $R_{4/2} = 2.024(4)$  and  $2.09(5)$ ] are close to the vibrational limit, suggesting a nearly spherical shape, whereas  $R_{4/2}$  for  $^{40}\text{Si}$  increases to  $2.56(5)$ , indicating a deviation from the spherical shape or enhancement of quadrupole collectivity at  $N = 26$ . The lowering of the  $2_1^+$  energy as well as the increase of the reduced transition probability or the deformation parameter obtained for  $^{36,38,40}\text{Si}$  was interpreted as a narrowing of the  $N = 28$  shell gap [12–14]. The prediction of the SM calculation using the recent SDPF-U-MIX interaction [33], an updated version of SDPF-U [18], is indicated by the dashed lines in Fig. 3. The new interaction, which allows  $np - nh$  excitations across the  $N = 20$  shell gap, reproduces  $E_x(2_1^+)$  and  $R_{4/2}$  in a satisfactory manner up to  $^{40}\text{Si}$ , but then deviates significantly from the experimental result for  $^{42}\text{Si}$  in Fig. 3(a). In the case of the  $N = 28$  isotope,  $E_x(2_1^+)$  is lower than  $^{40}\text{Si}$  and  $R_{4/2}$  further increases to  $2.93(5)$  despite the neutron magic number  $N = 28$ . This indicates that a development of nuclear deformation continues up to at least  $N = 28$ . In addition, the quadrupole collectivity increase in proton deficient  $N = 28$  isotones turns out to continue to  $^{42}\text{Si}$  with

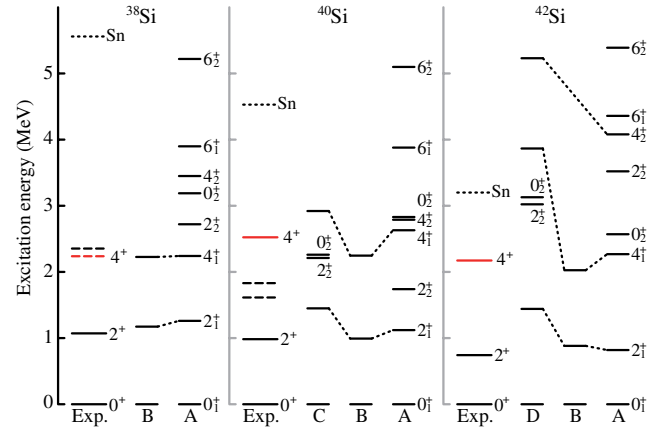


FIG. 4 (color online). Summary of the experimental and theoretical levels in  $^{38,40,42}\text{Si}$  isotopes. The dotted lines with the label  $S_n$  indicate the location of the experimental (for  $^{38,40}\text{Si}$ ) or evaluated (for  $^{42}\text{Si}$ ) neutron separation energy [34]. Among the experimental levels, the lines with red color indicate the new results from the present study. The labels A, B, C, and D represent, respectively, the results of the shell model calculations of Refs. [12,17,33], and the mean field calculation of Ref. [19].

$Z = 14$ . Thus, for  $^{42}\text{Si}$  well developed deformation has been experimentally established, and the possibility of a doubly magic nature has been excluded.

The solid lines in Fig. 3 indicate the results obtained by the SM calculation using the SDPF-MU interaction [17], which includes the tensor force in the effective interaction. The model reproduces the overall trends well, particularly for the  $4_1^+$  energies, where better agreement is achieved compared to SDPF-U-MIX. In particular, it predicts a large  $R_{4/2}$  value of 2.8 for  $^{42}\text{Si}$  which is close to the experimental result of  $2.93(5)$ . The mean field calculation with the relativistic energy density functional DD-PC1 [19] predicts a rotational band in  $^{42}\text{Si}$ . Though the excitation energies of the  $2_1^+$  and  $4_1^+$  states are about two times larger than the experimental values, the  $R_{4/2}$  ratio (2.7) is not far from the present result.

Figure 4 summarizes the experimental and theoretical level energies for the isotopes  $^{38,40,42}\text{Si}$ . The dashed lines indicate the levels observed in earlier studies [12,13] and the red lines show the  $4^+$  states tentatively assigned in the present study. The labels A, B, C, and D represent theoretical calculations by the SM with SDPF-MU [17], SM with SDPF-U-MIX [33], SM in Ref. [12], and mean field calculation [19], respectively. As seen in the figures, some model calculations predict more levels compared with the ones experimentally observed. The experimental energies of the calculated states with no empirical counterparts may provide a deeper understanding of nuclear structure. Together with possible measurements on  $\gamma$ -ray angular distributions and/or correlations, further efforts to identify those states present one target for future experiments with higher statistics by improvement of RI beam production. Other challenges on the experimental front, such as

measuring excited states in  $^{40}\text{Mg}$  and  $^{44}\text{Si}$ , are encouraged to further trace the quadrupole-collectivity development along the chains of  $N = 28$  isotones and  $Z = 14$  isotopes.

In summary, excited states in  $^{38,40,42}\text{Si}$  have been investigated via in-beam  $\gamma$ -ray spectroscopy with multi-nucleon removal reactions in inverse kinematics by using 210-MeV/nucleon  $^{40,44}\text{S}$  beams. With the high-efficiency detector array DALI2 and the high intensity secondary beams provided at RIKEN RIBF, measurements with high statistics were achieved. The energy of the first  $2^+$  state in  $^{42}\text{Si}$  was measured to be 742(8) keV, and the most probable candidate of the  $4_1^+$  state was found at 2173(14) keV with the aid of a  $\gamma - \gamma$  coincidence analysis. The  $4_1^+$  states in  $^{38}\text{Si}$  and  $^{40}\text{Si}$  were assigned excitation energies of 2239(25) and 2524(19) keV, respectively. The systematics of the ratio  $R_{4/2}$  of the  $4_1^+$  and  $2_1^+$  energies in silicon isotopes from  $N = 24$  to  $N = 28$  shows a rapid development of deformation. The  $R_{4/2}$  value of 2.93(5) for  $^{42}\text{Si}$  is the largest also among the known  $N = 28$  isotones, indicating that this nucleus is characteristic of a well-deformed rotor despite the magic numbers  $N = 28$  and  $Z = 14$ .

We thank the RIBF accelerator staff and the BigRIPS team for their valuable contributions to the experiment. We thank A. Poves for providing the new values and also Y. Utsuno and T. Otsuka for their calculations and discussions. This work was supported by the DFG (EXC 153, KR 2326/2-1), the U.S Department of Energy under Contracts No. DE-AC02-05CH11231 and No. DE-AC02-06CH11357, and the JUSEIPEN program.

\*takesato@riken.jp

†Present address: CNS, University of Tokyo, RIKEN Campus, Wako, Saitama 351-0198, Japan.

‡Present address: RCNP, Osaka University, Mihogaoka, Ibaraki, Osaka 567-0047, Japan.

§Present address: Institut für Kernphysik, Technische Universität Darmstadt, 64289 Darmstadt, Germany.

||Present address: TRIUMF, 4004 Wesbrook Mall, Vancouver, Canada.

¶Present address: Physik Department, Technische Universität München, D-85748 Garching, Germany.

\*\*Present address: ExtreMe Matter Institute EMMI and Research Division, GSI Helmholtzzentrum, 64291 Darmstadt, Germany.

††Present address: Los Alamos National Laboratory, Los Alamos, NM 87545, USA.

- [1] A. Navin *et al.*, *Phys. Rev. Lett.* **85**, 266 (2000).
- [2] H. Iwasaki *et al.*, *Phys. Lett. B* **481**, 7 (2000).
- [3] H. Iwasaki *et al.*, *Phys. Lett. B* **491**, 8 (2000).
- [4] C. Detraz, D. Guillemaud, G. Huber, R. Klapisch, M. Langevin, F. Naulin, C. Thibault, L. C. Carraz, and F. Touchard, *Phys. Rev. C* **19**, 164 (1979).
- [5] D. Guillemaud-Mueller, C. Detraz, M. Langevin, F. Naulin, M. De Saint-Simon, C. Thibault, F. Touchard, and M. Epherre, *Nucl. Phys. A* **426**, 37 (1984).

- [6] T. Motobayashi *et al.*, *Phys. Lett. B* **346**, 9 (1995).
- [7] E. K. Warburton, J. A. Becker, and B. A. Brown, *Phys. Rev. C* **41**, 1147 (1990).
- [8] O. Sorlin *et al.*, *Phys. Rev. C* **47**, 2941 (1993).
- [9] H. Scheit, T. Glasmacher, B. A. Brown, J. A. Brown, P. D. Cottle, P. G. Hansen, R. Harkewicz, M. Hellstrom, R. W. Ibbotson, J. K. Jewell, K. W. Kemper, D. J. Morrissey, M. Steiner, P. Thierolf, and M. Thoennessen, *Phys. Rev. Lett.* **77**, 3967 (1996).
- [10] T. Glasmacher, B. A. Brown, M. J. Chromik, P. D. Cottle, M. Fauerbach, R. W. Ibbotson, K. W. Kemper, D. J. Morrissey, H. Scheit, D. W. Sklenicka, and M. Steiner, *Phys. Lett. B* **395**, 163 (1997).
- [11] S. Grevy *et al.*, *Phys. Lett. B* **594**, 252 (2004).
- [12] C. M. Campbell *et al.*, *Phys. Rev. Lett.* **97**, 112501 (2006).
- [13] C. M. Campbell *et al.*, *Phys. Lett. B* **652**, 169 (2007).
- [14] R. W. Ibbotson, T. Glasmacher, B. A. Brown, L. Chen, M. J. Chromik, P. D. Cottle, M. Fauerbach, K. W. Kemper, D. J. Morrissey, H. Scheit, and M. Thoennessen, *Phys. Rev. Lett.* **80**, 2081 (1998).
- [15] J. Fridmann *et al.*, *Nature (London)* **435**, 922 (2005); *Phys. Rev. C* **74**, 034313 (2006).
- [16] B. Bastin, S. Grevy *et al.*, *Phys. Rev. Lett.* **99**, 022503 (2007).
- [17] T. Otsuka, T. Suzuki, and Y. Utsuno, *Nucl. Phys. A* **805**, 127c (2008); Y. Utsuno, T. Otsuka, B. A. Brown, M. Honma, T. Mizusaki, and N. Shimizu, [arXiv:1201.4077](https://arxiv.org/abs/1201.4077) [*Phys. Rev. C* (to be published)].
- [18] F. Nowacki and A. Poves, *Phys. Rev. C* **79**, 014310 (2009).
- [19] Z. P. Li, J. M. Yao, D. Vretenar, T. Niksic, H. Chen, and J. Meng, *Phys. Rev. C* **84**, 054304 (2011).
- [20] S. Takeuchi, T. Motobayashi, H. Murakami, K. Demichi, and H. Hasegawa, *RIKEN Accel. Prog. Rep.* **36**, 148 (2003).
- [21] S. Takeuchi *et al.*, *Phys. Rev. C* **79**, 054319 (2009).
- [22] T. Kubo, *Nucl. Instrum. Methods Phys. Res., Sect. B* **204**, 97 (2003).
- [23] P. Doornenbal *et al.*, *Phys. Rev. Lett.* **103**, 032501 (2009).
- [24] N. Kobayashi *et al.*, [arXiv:1111.7196](https://arxiv.org/abs/1111.7196) [*Phys. Rev. C* (to be published)].
- [25] Y. Mizoi, T. Kubo, H. Sakurai, K. Kusaka, K. Yoshida, and A. Yoshida, *RIKEN Accel. Prog. Rep.* **38**, 297 (2005).
- [26] H. Kumagai, A. Ozawa, N. Fukuda, K. Summerer, and I. Tanihata, *Nucl. Instrum. Methods Phys. Res., Sect. A* **470**, 562 (2001).
- [27] S. Agostinelli *et al.*, *Nucl. Instrum. Methods Phys. Res., Sect. A* **506**, 250 (2003).
- [28] S. Raman, C. W. Nestor, and P. Tikkanen, *At. Data Nucl. Data Tables* **78**, 1 (2001).
- [29] M. Bellegruic *et al.*, *Phys. Scr.* **T88**, 122 (2000).
- [30] K. Yoneda *et al.*, *Phys. Lett. B* **499**, 233 (2001).
- [31] P. Fallon *et al.*, *Phys. Rev. C* **81**, 041302 (2010).
- [32] X. Liang *et al.*, *Phys. Rev. C* **74**, 014311 (2006).
- [33] F. Rotaru, F. Negoita, S. Grévy, J. Mrazek, S. Lukyanov, F. Nowacki, A. Poves, O. Sorlin, C. Borcea, R. Borcea, A. Buta, L. Cáceres, S. Calinescu, R. Chevrier, Z. Dombrádi, J. M. Daugas, D. Lehbertz, Y. Penionzhkevich, C. Petrone, D. Sohler, M. Stanoiu, and J. C. Thomas, *Phys. Rev. Lett.* **109**, 092503 (2012).
- [34] <http://www.nndc.bnl.gov/nudat2/>, NuDat 2, nuclear structure and nuclear decay data.